# A Machine Learning-Assisted Framework to Control Thermally Anisotropic Building Envelopes in Residential Buildings

**Zhenglai Shen, PhD**
*Student Member ASHRAE*

**Som Shrestha, PhD**
*Member ASHRAE*

**Daniel Howard, PhD Student**
*Student Member ASHRAE*

**Tianli Feng, PhD**

**Diana Hun, PhD**
*Member ASHRAE*

**Buxin She, PhD Student**

## ABSTRACT

*To curb the energy consumption of buildings and their related $CO_2$ emissions, Oak Ridge National Laboratory (ORNL) developed the thermally anisotropic building envelope (TABE) —a multi-layer design comprising insulation materials and metal foils connected to thermal loops. This study developed a machine learning-assisted framework to control the TABE in residential buildings to reduce the computation load for future optimal rule-based control and application. First, a 2D finite element model was established in COMSOL to calculate the hourly heat flux through exterior walls installed with the TABE. Then, TABE wall heat fluxes were simulated for various indoor and outdoor boundary conditions, thermal loops fluid temperatures and flow rates. Since the finite element simulations are computationally expensive, an artificial neural network (ANN) was then trained to use as a proxy of the finite element (COMSOL) modeling. Finally, the trained ANN model was coupled with the EnergyPlus model to predict the energy consumption of a US Department of Energy prototype single-family house installed with the TABE. An optimal simple rule-based control was determined from predefined rules for a case study. The results demonstrate that the developed machine learning–assisted framework can reduce 99.9% of the computation time while efficiently managing residential building energy for installed TABE walls.*

## INTRODUCTION

In 2020, buildings accounted for 30% of global energy use and almost 14% of total direct energy-related $CO_2$ emissions (Hamilton and Rapf 2020). Therefore, it is urgent to curb the energy consumption of buildings and the related $CO_2$ emissions. Among the various building components, building envelopes are one of the most important components to manage building HVAC energy consumption. Both passive (Sadineni et al. 2011; Tian et al. 2018) and active (Luo et al. 2019) building envelope thermal management approaches have been studied to reduce unwanted heat flows passing through the envelopes. For passive building envelope thermal management, increasing R-value by adopting high-performance insulation materials such as vacuum insulation panels and aerogels has been extensively studied recently (Baetens et al. 2010, 2011; Biswas

Zhenglai Shen is a postdoc research associate at Oak Ridge National Laboratory (ORNL), Oak Ridge, Tennessee. Som Shrestha is a senior R&D staff at ORNL. Daniel Howard is a PhD student at University of Tennessee, Knoxville, and is working in ORNL. Tianli Feng is an assistant professor at University of Utah, Salt Lake City, Utah. Diana Hun is a group leader of Building Envelope Materials Research (BEMR) group at ORNL. Buxin She is a PhD student at the University of Tennessee, Knoxville.

2018). However, high cost and durability issues limit their application in building envelopes (Biswas et al. 2019a). Additionally, increasing the thermal mass of building envelopes by incorporating phase change materials has also shown the potential to reduce heating/cooling loads (Biswas et al. 2018; Kośny et al. 2014). However, there is a lack of large-scale applications to show its feasibility. For active building envelope thermal management, the concepts of the active evaporative cooling wall (Carbonari et al. 2015), dynamic insulation system (Dabbagh and Krarti 2020), and active photovoltaic-thermoelectric wall system (Liu et al. 2015b; a) have been studied. Similarly, they lack feasibility, and the research only focused on numerical studies.

Recently, researchers at the US Department of Energy's (DOE's) Oak Ridge National Laboratory developed a thermally anisotropic building envelope (TABE) (Biswas et al. 2019a; b; Shrestha et al. 2020) to improve the thermal management in building envelopes. The TABE allows heat to dissipate in a preferential direction by sandwiching highly thermally conductive thin metal sheets, such as aluminum, between insulation layers. The TABE wall panel has nominal 2 × 4 in. studs (actual 1.5 in. × 3.5 in. [ 3.8 cm × 8.9 cm] at 16 in. [40.6 cm] on the center, interior ½ in. gypsum board, R-13 (13 h.ft$^2$.°F/Btu [2.23 m$^2$.K/W]) fiberglass batt insulation in the cavities, two layers of ½ in. [1.3 cm] Polyiso, and exterior horizontal vinyl siding as shown in Figure 1. The wall panel assemblies meet the International Energy Conservation Code 2018 R-value requirements for a residential building wall in ASHRAE climate zones 3 to 5. To accelerate the heat dissipation rates, interior and exterior thermal loops were integrated into the TABE. When connecting to a groundwater loop, the TABE wall panel can be used as: (1) a heat sink to separate the indoor environment from the influence of the outdoor when activating the exterior thermal loop; or (2) a heating/cooling source when activating the interior thermal loop with suitable ground water temperature. Laboratory evaluations showed that the TABE can reduce 85% of cooling loads and 63% of heating loads (Biswas et al. 2019a). Similar cooling and heating load reductions were observed in a series of field evaluations.

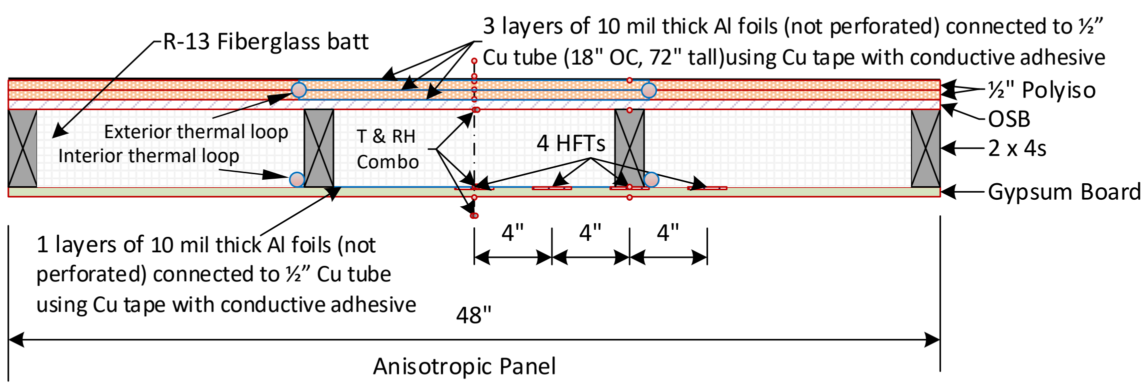


**Figure 1** Schematic of a prototype TABE panel with both interior and exterior thermal loops

To assist experimental efforts, COMSOL and EnergyPlus models were developed to simulate the energy savings of residential buildings installed with TABE walls. A COMSOL finite element model (FEM) was used to simulate the heat flux and thermal performance of TABE walls. The outputs of COMSOL were then used as the inputs to EnergyPlus to simulate the whole building's energy consumption. The COMSOL models were calibrated using the data collected by field evaluation. However, the COMSOL simulations were extremely time-consuming because of the geometric complexity of TABE walls. For example, COMSOL required about 2 days to compute the annual heat flux for a given water flow rate and thermal loop setting. Such a relatively long computation time made it difficult to test the performance of predefined control rules using a FEM such as COMSOL. More importantly, it prevented the integration of optimization algorithms and more advanced control algorithms, such as model predictive control into the studies of buildings installed with TABE walls. For example, the application of an optimization algorithm (e.g., multi-objective particle swarm optimization) to find an optimal control rule may involve thousands of heat flux computations of TABE walls, which will be an impossible task using the physics-based model. Therefore, an efficient surrogate model is needed, such as an artificial neural network (ANN) model, to substitute for the computationally expensive physics-based FEM.

This study addressed the need for an efficient surrogate model by developing a machine learning–assisted framework to replace the computationally expensive FEM to control the TABE in residential buildings and reduce energy consumption. First, a 2D FEM of the TABE panel was established in COMSOL to calculate the hourly heat flux subject to indoor and outdoor boundary conditions with tunable inlet water flow rate and temperature in the thermal loops. An ANN model was then trained to substitute the computationally expensive COMSOL model. After that, the trained ANN model was integrated with EnergyPlus to simulate the thermal performance of residential buildings. Finally, an optimal simple rule-based control was determined from predefined rules for a case study for a DOE prototype single-family house.

## METHODOLOGY

The machine learning–assisted, rule-based control framework to manage residential building energy consumption with a hydraulic activated TABE is shown in Figure 2. The framework includes four stages.
*Stage 1*: TABE wall heat fluxes are output from FEM simulations based on specific boundary conditions, which are generated by a baseline EnergyPlus model, and various constant TABE water flow rates as the inputs.
*Stage 2*: An ANN is trained based on the outputs from Stage 1. The ANN can predict TABE wall heat fluxes for any given climate conditions and TABE water flow rates.
*Stage 3*: Using the ANN, TABE wall heat fluxes are predicted based on the Time-Of-Days (TODs) with different control strategies. These TODs influence the water flow rate schedules used as inputs to the ANN.
*Stage 4*: Using the ANN predicted TABE wall heat fluxes, the energy consumption of buildings is calculated in EnergyPlus.

The developed framework was applied to a DOE prototype single-family residential building in Charleston, South Carolina (Climate Zone 3A).

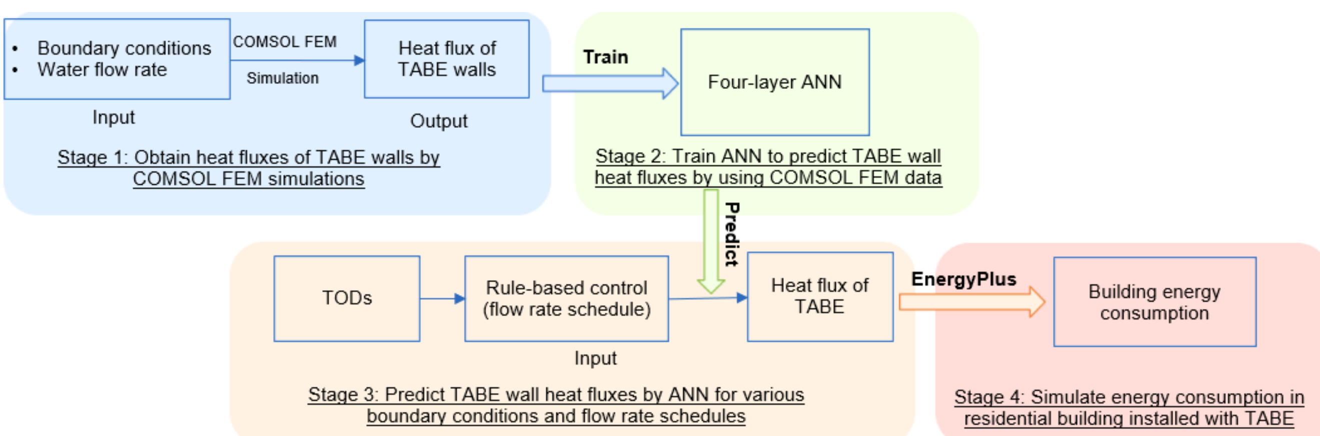


**Figure 2** Machine learning–assisted rule-based control framework to manage residential building energy consumption with the hydronic activated TABE

### FEM simulation of TABE wall heat fluxes: Training Data Preparation

FEM simulations were conducted via COMSOL to calculate TABE wall heat fluxes for given climate conditions and various constant water flow rates. The obtained TABE wall heat fluxes data were used as the training data for the ANN. A 2D

3

COMSOL model was adopted because it greatly reduced the computation load compared with the 3D model. However, the computation time of the 2D model is still not affordable if used in parametric studies, such as looking for the optimal control rules to minimize annual energy consumption for given climate conditions. The inputs and outputs of the 2D model are listed in Table 1. They include 11 input variables and 1 output for each wall (4 walls for the studied single-family residential building). Only a representative area (10.76 ft$^2$ [1 m$^2$]) of the TABE was simulated for each wall; then, the area was scaled up to the entire opaque wall area of the prototype building. The wall surface temperature, air temperature, and radiation heat flux inputs were obtained from a baseline EnergyPlus model that has identical construction to the TABE walls but without metal layers and thermal loops. The groundwater temperature was obtained from the US Geological Survey database. In this study, the interior and exterior thermal loops were computed separately.

The characteristic temperatures of Charleston are provided in Table 2. It has a cold winter and hot summer with suitable groundwater temperature (66°F [19°C]).

**Table 1. Inputs and Outputs of COMSOL Model**

| Inputs and Outputs | Variables |
|---|---|
| Inputs | (1) Interior wall surface temperature; (2) Exterior wall surface temperature; (3) Indoor air temperature; (4) Outdoor air temperature; (5) Interior wall surface convection coefficient; (6) Exterior wall surface convection coefficient; (7) Inside surface radiation; (8) Surface outside face net thermal radiation heat gain rate; (9) Surface outside face solar radiation heat gain rate; (10) Ground water temperature; (11) Water flow rate |
| Outputs | (1) Heat flux from the walls to the conditioned space |

**Table 2. Characteristic Temperatures of Charleston**

| | AAGWT* °F (°C) | Min OAT** °F (°C) | Max OAT** °F (°C) | Avg OAT** °F (°C) |
|---|---|---|---|---|
| Temperature | 66.2 (19.0) | 21.9 (-5.6) | 100 (37.8) | 65.3 (18.5) |

*AAGWT = Annual average ground water temperature
**OAT = Outdoor air temperature

## ANN

ANNs have a strong fitting capability owing to their thousands of neurons and nonlinear activation functions. An ANN may represent a wide variety of functions when given appropriate weights and biases (Scarselli and Chung Tsoi 1998). In this study, a multilayer perception (MLP) (Mohandes et al. 2019) was used to predict TABE wall heat fluxes based on 11 inputs as listed in Table 1. Hourly data were used in training the ANN model. For Charleston, a dataset with a sample size of 175,200 (8,760 simulated hours × 4 walls × 5 different water flow settings) was generated. The 5 different water flow settings include a baseline without water flow, interior thermal loop with 0.1 GPM, exterior thermal loop with 0.1 GPM, interior thermal loop with 0.5 GPM, and exterior thermal loop with 0.5 GPM. To discrete the differences of interior and exterior thermal loops in training the ANN, a minus sign was added to indicate the exterior thermal loop. For example, -0.1 GPM presents that the TABE wall runs the exterior thermal loop with 0.1 GPM. Considering the large data set, the MLP was configured to have 2 hidden layers (as shown in Figure 1), each with 512 neurons. It was then randomly initialized with a standard deviation of 0.01 for weights and trained with a stochastic gradient descent (SDG) optimizer. In addition, rectified linear unit (ReLU) was used as activation function, 0.05 was used as the learning rate, 128 was used as the batch size, and 200 was used as the number of epochs. An epoch is one complete pass of the training data set through the algorithm, which can be viewed as an iteration of the machine learning training process. After extensive offline training, the MLP can be implemented online along with water flow rate control algorithms to help manage residential building energy consumption.

### Rule-based Control Design

The rule-based control strategies were designed according to the control modes of the TABE system and the TODs. Three modes were considered, as described in Table 3, where each mode only includes complementary “ON” and “OFF” settings from the remaining two other modes. TOD has been used to generate optimal control rules according to TOD tariffs, especially for buildings installed with a thermal energy storage system (Kamal et al. 2019). The concept was applied to design the control rules because the outdoor climate conditions were different in each TOD, so TOD can be used as an indicator to activate/inactivate thermal loops of TABE. The day was divided into five TODs, which include the early morning period, morning period, on-peak period, evening period, and late evening period, as described in Table 4.

**Table 3. Control Modes of the TABE System**

| Control Modes | Description |
|---|---|
| Mode 1 | Interior thermal loop is ON and exterior thermal loop is OFF |
| Mode 2 | Interior thermal loop is OFF and exterior loop is ON |
| Mode 3 | Interior loop is OFF and exterior loop is OFF |

**Table 4. TODs**

| TODs | Description |
|---|---|
| TOD 1 | Early morning period (2:00 to 6:00 a.m.) |
| TOD 2 | Morning period (6:00 to 10:00 a.m.) |
| TOD 3 | On peak period (10:00 a.m. to 5:00 p.m.) |
| TOD 4 | Evening period (5:00 to 10:00 p.m.) |
| TOD 5 | Late evening period (10:00 p.m. – 2:00 a.m.) |

According to the defined control models and TODs, four control rules were generated (Figure 3), where two different series of control rules were developed based on different seasons. For the cooling season (April to October), it is desired to run the interior thermal loop during the daytime (TOD 2 and TOD 3) to gain the cooling energy from cold groundwater and run the exterior thermal loop during the evening period (TOD 4) to isolate the indoor environment from outdoor ground thermal radiation. In TOD 1 and TOD 5, the thermal loops can be turned off to precool the building. Therefore, two control rules were designed: cooling (Rule 1) and pre-cooling (Rule 2) in the early morning period, as shown in Figure 3(a). Similar reasoning was used to design control rules for the heating season (November to March).

The developed machine learning assisted framework was implemented in Building Control Virtual Test Beds (BCVTB) (Wetter 2010). The trained ANN and control rules were implemented in MATLAB which could be directly called by BCVTB in each time-step for building energy consumption analysis in EnergyPlus.

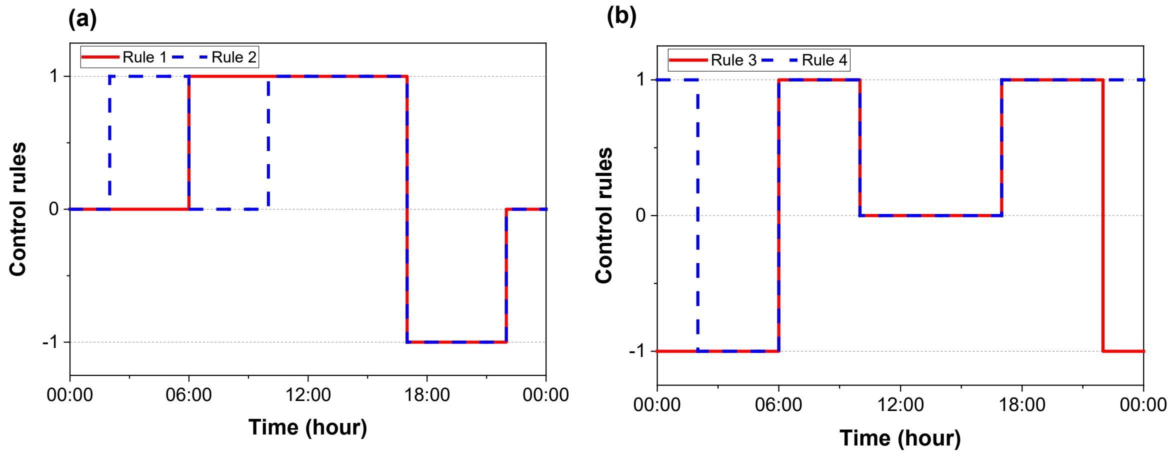


**Figure 3** (a) control rules of TABE thermal loop for months April to October (cooling season); (b) control rules of TABE thermal loops for months November to March (heating season).

## RESULTS AND DISCUSSION

### ANN Training results

The ANN with two hidden layers was trained with 80% of samples and 20% of samples for validation and testing. Figure 4 shows the mean squared error (MSE) loss of the ANN predictions. For the training set, the ANN shows a 0.2 MSE loss at 200 epochs (Figure 4 (a)), which is reasonably good. Although a smaller MSE loss is achievable, it may lead to overfitting. For the test set, a similar MSE loss was obtained, which indicates that the four-layer ANN performs consistently. In addition, the result shows the test error was nested around zero with an overall MSE of 23%, which indicates acceptable accuracy, see Figure 4 (b), although it has a <20% prediction error for about 60% of the test samples. The training accuracy of the ANN can be improved by either including more flow rates (e.g., 0.3 GPM [0.069 $m^3/h$]) or considering a more suitable neural network for time series data such as the recurrent neural network. The trained ANN model was applied in MATLAB, which can be integrated into BCVTB at each timestep for the energy co-simulation. The calculation time of heat flux by using the trained ANN model was significantly reduced compared with the FEM simulations in COMSOL, from 2 days to less than 1 min (99.9% time saving), which makes future efforts on finding optimal rules using an optimization algorithm more feasible.

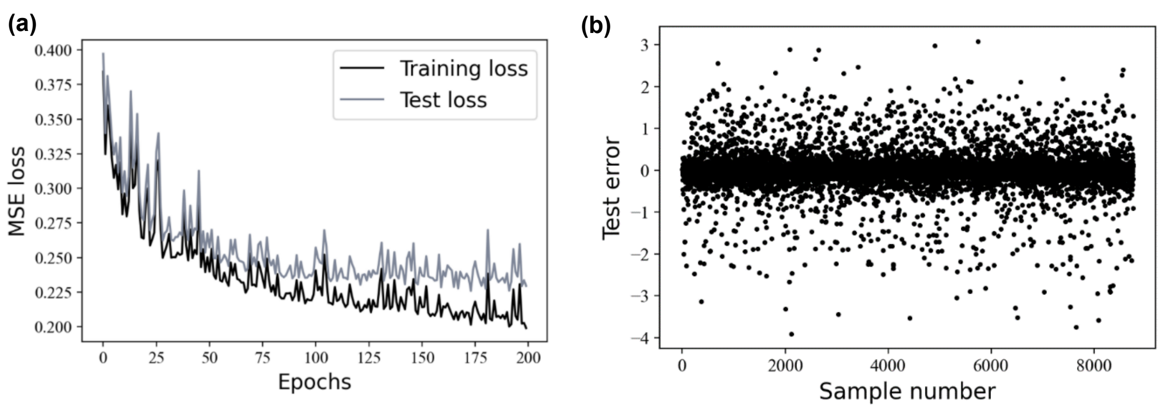


**Figure 4** (a) MSE training and test losses; (b) test error.

## Annual Energy Consumption, Cost, and Heat Flux Behavior

The annual HVAC energy cost and savings for the case study building with various water flow rates and rule combinations are presented in Figure 5. The annual HVAC energy cost was calculated by using the electricity (cooling) and natural gas (heating) consumption (as described in Table 5) multiplied by their corresponding unit price—$0.13/kWh for electricity and $0.063/kWh for natural gas. The studied cases were labeled by the selected control rules and water flow rates, where the control rules label cooling and heating seasons. For example, "Rule13" represents that Rule 1 was used for the cooling season, and Rule 3 was used for the heating season. "WR0.1" represents the water flow rate is 0.1 GPM. In addition, constant water flow rates of 0.1, 0.15, and 0.2 GPM (0.023, 0.034, and 0.045 $m^3/h$) with pump powers of 33.0, 34.0, and 35.7 W are considered in the annual energy consumption and cost analysis.  The buildings with the TABE buildings have greatly reduced annual HVAC energy cost compared with the baseline building without the TABE. More than 9% of the HVAC energy cost was saved in all the studied cases, and Rule13_WR0.15 reached the highest cost saving of 17.4%. On the other hand, Rule13_WR0.1 reached the highest energy consumption savings (see Table 5) because of the relatively higher price of electricity, whereas Rule14_WR0.15 had more electricity cost savings. This study did not consider the energy consumption required to run the pumps of thermal loops, where a higher water flow rate consumes more electricity. Therefore, Rule13_WR0.1 is the optimal rule among the predefined rules.

The energy cost savings come from the HVAC electricity savings (cooling season) but with a slightly higher natural gas consumption (heating season), as shown in Table 5. This is mainly because overcooling happens during the cooling season which requires using heating energy (natural gas) to balance it. The annual heat flux behavior of the south wall and the annual net heat gain/loss during cooling/heating hours are shown in Figure 6. Clearly, the adoption of the TABE leads to a negative net heat gain during the cooling season. This indicates that the TABE wall will help to maintain the indoor environment by supplying cooling energy instead of consuming it as its counterpart of the baseline case. However, the current rule-based control did not overcome the issue of overcooling due to the relatively low temperature of the groundwater (see Table 2). This phenomenon was confirmed by analyzing the net heat gain/loss during cooling/heating hours, where buildings with the TABE walls lead to less heat loss compared with the baseline case during the heating season, as shown in Figure 6(b). Therefore, future research is needed to combine the developed framework and optimization algorithms to find optimal control rules that can address the observed overcooling issue. The cost savings by the TABE by using an optimal control rule could likely be much higher than 20% compared with the baseline case.

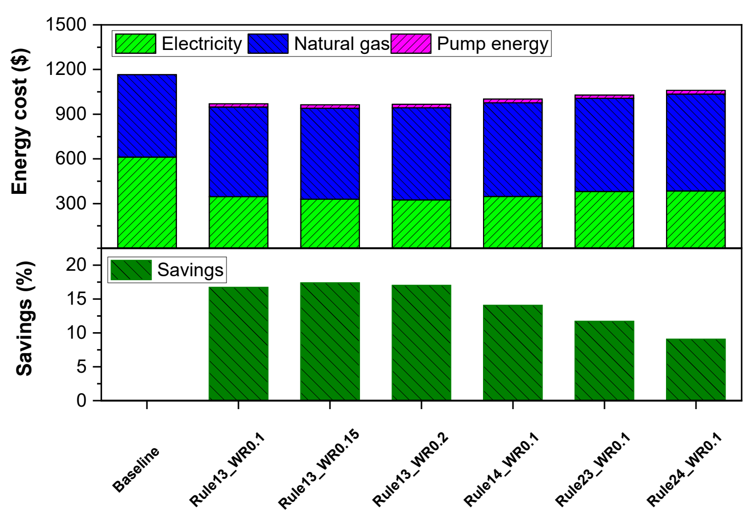


**Figure 5** Annual HVAC and pump energy cost and savings for Charleston for different cases

**Table 5. Annual Energy Consumptions of Different Cases**

| Energy (kWh) | Baseline | Rule13_ WR0.1 | Rule13_ WR0.15 | Rule13_ WR0.2 | Rule14_ WR0.1 | Rule23_ WR0.1 | Rule24_ WR0.1 |
|---|---|---|---|---|---|---|---|
| Electricity | 4,484 | 2,539 | 2,420 | 2,380 | 2,555 | 2,799 | 2,816 |
| Pump electricity | 0 | 163 | 168 | 176 | 179 | 163 | 179 |
| Natural gas | 8,776 | 9,538 | 9,665 | 9,797 | 9,961 | 9,898 | 10,321 |
| Total | 13,260 | 12,240 | 12,253 | 12,354 | 12,695 | 12,860 | 13,316 |

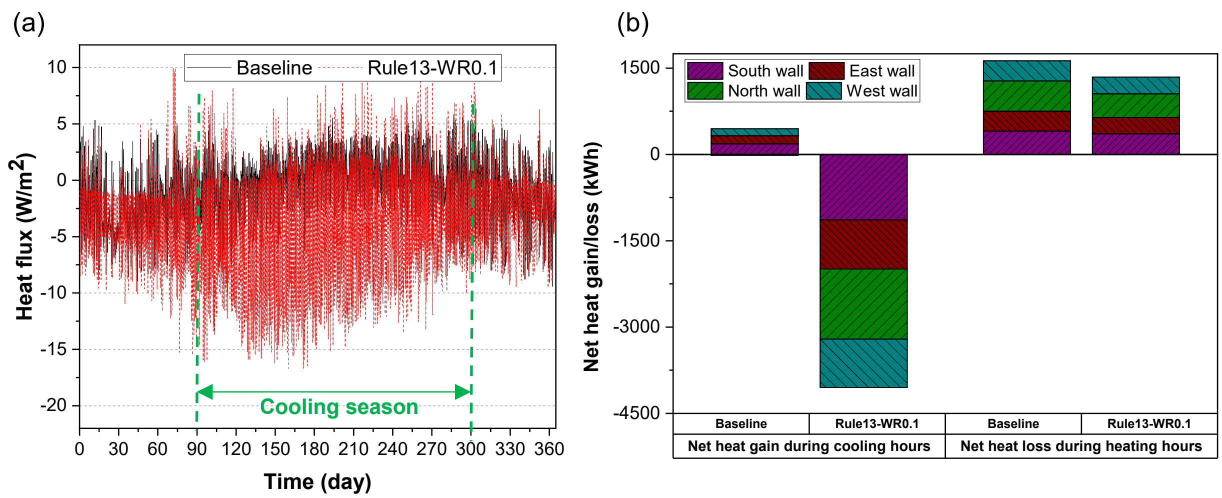


**Figure 6** Annual interior surface heat flux and net heat gain/loss: (a) annual interior surface heat flux of the south wall; (b) annual net heat gain/loss during cooling/heating hours.

## CONCLUSIONS AND FUTURE RESEARCH

In this study, a machine learning–assisted framework to control the TABE in residential buildings was developed, and an ANN model was trained to reduce the high computation cost of the FEM simulations of the TABE systems. The framework was applied in BCVTB to calculate the energy consumption of a DOE prototype residential building in Charleston, South Carolina, using different rule-based controls. The following conclusions are drawn:

1. The ANN model has a reasonable accuracy to substitute the physics-based FEM simulations of the TABE. However, the training and test accuracy may need to be further improved in future research.
2. The computation time was greatly reduced from 2 days for a single case FEM simulation by COMSOL for the annual analysis, to less than 1 min by using the ANN, indicating 99.9% savings in computation time. Such an improvement makes future studies in finding optimal control rules more feasible.
3. The case study shows that the designed control rules based on TOD have great potential to reduce the annual energy cost of residential buildings installed with TABE walls.

Future research can target the following efforts:

1. Extend this study to other climate zones to increase the variability of the training samples.
2. Use an optimization algorithm to identify the most suitable TOD for the cooling and heating season. Meanwhile, overcooling will be addressed in the optimization process by considering the heating/cooling demands in each time step.
3. Increase the accuracy of the machine learning model by using a recurrent neural network, which is more suitable for time series data.

## ACKNOWLEDGEMENTS

This manuscript has been authored in part by UT-Battelle, LLC, under contract DE-AC05-00OR22725 with the US Department of Energy (DOE). The publisher acknowledges the US government license to provide public access under the DOE Public Access Plan (http://energy.gov/downloads/doe-public-access-plan). The authors thank Sven Mumme for his support and guidance and Olivia Shafer for formatting and technical editing.

## REFERENCES


Baetens, R., B. P. Jelle, and A. Gustavsen. 2011. “Aerogel insulation for building applications: A state-of-the-art review.” *Energy Build.*, 43 (4): 761–769. Elsevier B.V. https://doi.org/10.1016/j.enbuild.2010.12.012.

Baetens, R., B. P. Jelle, J. V. Thue, M. J. Tenpierik, S. Grynning, S. Uvsløkk, and A. Gustavsen. 2010. “Vacuum insulation panels for building applications: A review and beyond.” *Energy Build.*, 42 (2): 147–172. https://doi.org/10.1016/j.enbuild.2009.09.005.

Biswas, K. 2018. “Development and validation of numerical models for evaluation of foam-vacuum insulation panel composite boards, including edge effects.” *Energies*, 11 (9). https://doi.org/10.3390/en11092228.

Biswas, K., S. Shrestha, D. Hun, and J. Atchley. 2019a. “Thermally Anisotropic Composites for Improving the Energy Efficiency of Building Envelopes.” *energies*.

Biswas, K., S. Shrestha, D. Hun, and J. Atchley. 2019b. “Thermally Anisotropic Composites for Heat Redirection and Thermal Management in Building Envelopes.” *2019 Therm. Perform. Exter. Envel. Whole Build. XIV Int. Conf.* Clearwater, Florida.

Biswas, K., Y. Shukla, A. Desjarlais, and R. Rawal. 2018. “Thermal characterization of full-scale PCM products and numerical simulations, including hysteresis, to evaluate energy impacts in an envelope application.” *Appl. Therm. Eng.*, 138 (April): 501–512. Elsevier. https://doi.org/10.1016/j.applthermaleng.2018.04.090.

Carbonari, A., B. Naticchia, and M. D. Orazio. 2015. “Innovative evaporative cooling walls.” *Eco-Efficient Mater. Mitigating Build. Cool. Needs*, 215–240.

Dabbagh, M., and M. Krarti. 2020. “Evaluation of the performance for a dynamic insulation system suitable for switchable building envelope.” *Energy Build.*, 222: 110025. Elsevier B.V. https://doi.org/10.1016/j.enbuild.2020.110025.

Hamilton, I., and O. Rapf. 2020. “E2020 global status report for buildings and construction: towards a zero-emissions, efficient and resilient buildings and contruction sector.” *Glob. Alliance Build. Constr.*, 1–7.

Kamal, R., F. Moloney, C. Wickramaratne, A. Narasimhan, and D. Y. Goswami. 2019. “Strategic control and cost optimization of thermal energy storage in buildings using EnergyPlus.” *Appl. Energy*, 246 (August 2018): 77–90. Elsevier. https://doi.org/10.1016/j.apenergy.2019.04.017.

Kośny, J., A. Fallahi, N. Shukla, E. Kossecka, and R. Ahbari. 2014. “Thermal load mitigation and passive cooling in residential attics containing PCM-enhanced insulations.” *Sol. Energy*, 108: 164–177. https://doi.org/10.1016/j.solener.2014.05.007.

Liu, Z., L. Zhang, G. Gong, and T. Han. 2015a. “Experimental evaluation of an active solar thermoelectric radiant wall system.” *Energy Convers. Manag.*, 94: 253–260. Elsevier Ltd. https://doi.org/10.1016/j.enconman.2015.01.077.

Liu, Z., L. Zhang, G. Gong, Y. Luo, and F. Meng. 2015b. “Evaluation of a prototype active solar thermoelectric radiant wall system in winter conditions.” *Appl. Therm. Eng.*, 89: 36–43. Elsevier Ltd. https://doi.org/10.1016/j.applthermaleng.2015.05.076.

Luo, Y., L. Zhang, M. Bozlar, Z. Liu, H. Guo, and F. Meggers. 2019. “Active building envelope systems toward renewable and sustainable energy.” *Renew. Sustain. Energy Rev.*, 104 (July 2018): 470–491. Elsevier Ltd. https://doi.org/10.1016/j.rser.2019.01.005.

Mohandes, S. R., X. Zhang, and A. Mahdiyar. 2019. “A comprehensive review on the application of artificial neural networks in building energy analysis.” *Neurocomputing*, 340: 55–75. Elsevier B.V. https://doi.org/10.1016/j.neucom.2019.02.040.

Sadineni, S. B., S. Madala, and R. F. Boehm. 2011. “Passive building energy savings: A review of building envelope components.” *Renew. Sustain. Energy Rev.*, 15 (8): 3617–3631. https://doi.org/10.1016/j.rser.2011.07.014.

Scarselli, F., and A. Chung Tsoi. 1998. “Universal approximation using feedforward neural networks: A survey of some existing methods, and some new results.” *Neural Networks*, 11 (1): 15–37. https://doi.org/10.1016/S0893-6080(97)00097-X.

Shrestha, S., K. Biswas, D. Hun, and J. Atchley. 2020. “Thermally Anisotropic Composites for Thermal Management in Building Environments.” USA.

Tian, Z., X. Zhang, X. Jin, X. Zhou, B. Si, and X. Shi. 2018. “Towards adoption of building energy simulation and optimization for passive building design: A survey and a review.” *Energy Build.*, 158: 1306–1316. Elsevier B.V. https://doi.org/10.1016/j.enbuild.2017.11.022.

Wetter, M. 2010. *Building Controls Virtual Test Bed User Manual Version 0.8.0. Lawrence Berkeley Natl. Lab.*